

In silico analysis of microdomain-mediated trimer formation in the T cell membrane

E. Long^{1,2,a}, B. Henderson³, and A. Zaikin^{2,4}

¹ CoMPLEX, University College London (UCL), Gower St, London, UK

² Department of Mathematics, UCL

³ Division of Microbial Diseases, UCL Eastman Dental Institute

⁴ Institute for Women's Health, UCL

Received 03 August 2010 / Received in final form 09 August 2010
Published online 01 October 2010

Abstract. We consider stochastic reaction-diffusion dynamics involved in the formation of a trimeric protein receptor complex, where diffusion is modulated by the presence of small, fixed membrane microdomains. Compartmentalisation of cell membrane signalling proteins may optimise signal transduction but previous modelling work suggests that signalling is only augmented if microdomains are highly mobile. Using a Gillespie algorithm-based spatial numerical simulation, we examine the effect of the presence, size and total coverage of microdomains, which either slow protein diffusion or trap proteins at their boundary. We examine scenarios where protein-protein interactions take place within microdomains, and also where interactions are favoured at the microdomain boundary. This model is motivated by the formation of the high-affinity receptor for the cytokine IL-2. Proliferation requires a threshold number of bound receptors, but pleiotropic effects of IL-2 on other cell types means that high ligand concentrations are undesirable. Hence, optimising T cell sensitivity to IL-2 is essential. In agreement with earlier models, we find that small microdomain sizes result in the greatest augmentation in receptor formation, but that static microdomains can also confer an increased sensitivity in the case of heterotrimeric receptor complex formation.

1 Introduction

Compartmentalisation is central to biology. Multicellular organisms delegate key processes to specialised organs, themselves composed of various distinct tissues. These are, in turn, composed of cells, each adapted to fulfil its own function. At the subcellular level, lipid membranes partition the cell into distinct organelles, controlling the passage of functional molecules from organelle to organelle, and from the inside of the cell to the outside.

Since 1997, compartmentalisation in the lipid membranes themselves has come under scrutiny. This was in response to a review paper in *Nature* by Simons & Ikonen [1] suggesting that small areas in the cell membrane enriched in cholesterol and saturated lipids (membrane *microdomains* or *rafts*) might act as protein sorting platforms regulating cell signalling and trafficking.

Membrane protein organisation is critical in signalling by cells involved in the immune response. In the formation of the T cell receptor (TCR), for example, lipid and protein species are coordinated to a single area where the T cell comes into contact with an antigen-presenting cell (APC) [2–4]. The TCR is an example of membrane compartmentalisation on a fairly large

^a e-mail: e.long@ucl.ac.uk

scale, but smaller microdomain-mediated sorting of component proteins in order to form larger receptor complexes could be important in optimising the sensitivity of cells to low-concentration immunostimulatory signals in order to effect a timely and proportionate response.

We are interested here in the organisation of the trimeric membrane receptor for the short-range cell signalling molecule (cytokine) interleukin 2 (IL-2). IL-2 is a signalling molecule expressed by T cells in response to TCR binding and is involved in the activation and proliferation of cytotoxic T cells as well as the maintenance of populations of regulatory T cells (T_{reg} cells) [5]. T_{reg} cells suppress immune activation, maintaining immune system homeostasis. This system is of interest because there exists relatively little modelling of multi-component membrane receptor organisation involving microdomains and because controlling sensitivity of T cells to IL-2 ligand is of interest in therapies for immune deficiency and leukaemia.

2 Compartmentalisation in lipid membranes

The model in which protein species are distributed essentially randomly in the membrane was termed the *fluid mosaic model* after a 1972 paper by Singer and Nicholson [6]. Recent evidence, however, points to a degree of lateral heterogeneity in the distribution of both proteins and lipids whereby patches of the membrane are enriched in certain species and, rather than migrating freely throughout the membrane, protein diffusion may be constrained by interaction with the lipid environment, other membrane proteins or cytoskeletal components.

Studies in cholesterol-enriched model membranes show phase separation into liquid-ordered and liquid-disordered domains on the scale of several micrometers [7]. *In vivo*, domains of this scale are not ordinarily observed, but evidence for lateral segregation of lipid and protein species on a smaller scale (around 10–100 nm) exists based on methods such as fluorescence resonance energy transfer (FRET), fluorescence recovery after photobleaching (FRAP), atomic force microscopy (AFM) and single-particle tracking (SPT) [8].

Computational and mathematical approaches have shed light on the dynamics of membrane organisation [9, 10] and the role of lateral segregation in protein sorting. Pandit [11] and, more recently, Risselada & Marrink [12] have shown spontaneous phase separation into distinct domains in near-atomic scale simulations of ternary lipid mixtures; the latter are working on models of diffusion of the membrane-integrated syntaxin proteins. Nudelman et al. created a Monte Carlo simulation to probe the influence of lipid microdomains on B cell receptor interactions with multivalent ligands [13].

Nicolau et al. [14] constructed a stochastic model to determine ‘optimal’ characteristics of membrane microdomains in terms of their individual size and total membrane coverage. The authors measured the number of collisions within a population of diffusing ‘protein’ particles and the proportion of proteins which were sorted into microdomains. They found the proportion of proteins sorted into microdomains was highest when the ratio of the diffusion rate inside microdomains relative to the rate outside the microdomains was low and when the total microdomain coverage was high. Furthermore, the protein-protein collision rate was almost unaffected by the presence of microdomains unless the microdomains were mobile but, when mobile microdomains were present, there existed an ‘optimal’ microdomain radius which maximised the collision rate.

In this study, we examine a system where three distinct diffusing protein species interact to form a trimeric complex. We determine the influence of microdomain characteristics and affinities between microdomains and diffusing proteins on the equilibrium state of the system.

3 Formation of the IL-2 receptor

The IL-2 receptor (IL-2R) is a complex made up of three subunits termed α , β , and γ . The subunits of the receptor are involved in diverse signalling pathways: the γ subunit is also involved in transducing signals initiated by the binding of at least six other cytokines: IL-4, IL-7, IL-9, IL-15 and IL-21 [15]. In the case of IL-15, the β subunit is also part of the receptor complex

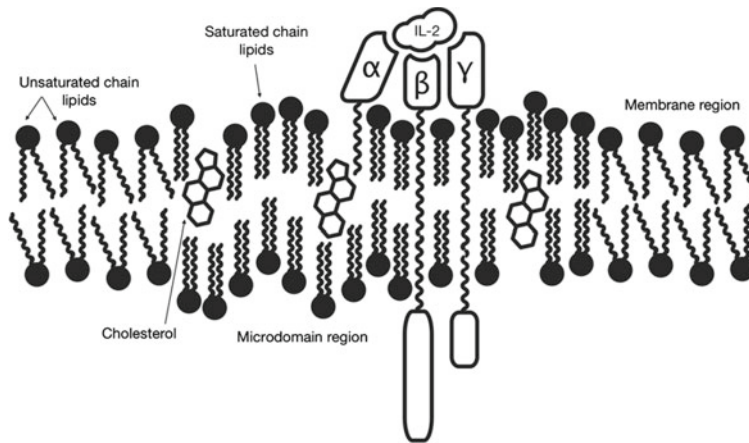


Fig. 1. A cross section of the membrane, showing a microdomain region containing mainly saturated chain lipid molecules and cholesterol with a bound trimeric IL-2 receptor. The α subunit is inserted only into the outer leaflet of the membrane, whereas the β and γ subunits contain long, transmembrane domains.

and there is a distinct IL-15R α component which makes up the trimer. Although both IL-2 and IL-15 can signal through the partially formed $\beta\gamma$ complex, the addition of the α subunit increases the affinity of the ligand binding [16]. Thus there is competition between the two cytokines at two levels: both compete to bind to the $\beta\gamma$ receptor and the IL-2R α and IL-15R α subunits compete to form a complete heterotrimer in order to bind their ligand with high affinity. In this type of system, the sorting of component proteins in the membrane could be crucial in determining whether the cell responds to an IL-2 or IL-15 signal as each cytokine has the potential to block signalling by the other.

There is evidence that sorting of membrane proteins is involved in receptor formation: subunits have been found associated with membrane microdomains both by detergent extraction methods and FRET co-localisation measurements. Exactly which subunits are microdomain-associated, however, varies in different investigations. Matkó et al. found all three subunits of the IL-2 receptor in the detergent-resistant (microdomain) fraction, both in the presence and absence of IL-2 ligand. FRET efficiency measurements also indicated co-localisation between all subunits and microdomain-associated proteins including CD48 [17, 18]. An independent study by Goebel et al., however, examined the distribution of the subunits of the IL-2R and IL-15R and found only the β subunit expressed in the detergent-resistant fraction [19]. On ligation, there was partial translocation of the β subunit into the membrane fraction. A third investigation by Marmor & Julius found only the IL-2R α subunit enriched in the microdomain fraction [20].

The balance between the two downstream pathways initiated by binding IL-2 or IL-15 ligand is a system of some complexity and the involvement of protein sorting would add further detail. As such, predicting the behaviour of a cell in response to competing IL-2 and IL-15 stimuli is not at all straightforward. Constructing models of the dynamics of the component proteins provides a tool quantitatively to assess how a cell responds to its environment in this situation.

Based on *in vitro* assays, IL-2 was assumed to be essential to T cell proliferation in response to TCR binding. Later studies with both IL-2 and IL-2R α double knockouts, however, did not result in the expected impairment of the proliferative response in a murine model. This result led to the hypothesis that there were redundant growth factors active *in vivo* which could replace the IL-2 signalling pathway. IL-2 does play a role in managing the function of immune cells, however: mice unable to express IL-2 later develop autoimmune problems and an accumulation of activated CD4⁺ cells [21]. Thus, the function of IL-2 is twofold: as well as inducing proliferation in activated T cells, it also sensitises them for activation-induced cell death in order to self-limit the scale of the immune response.

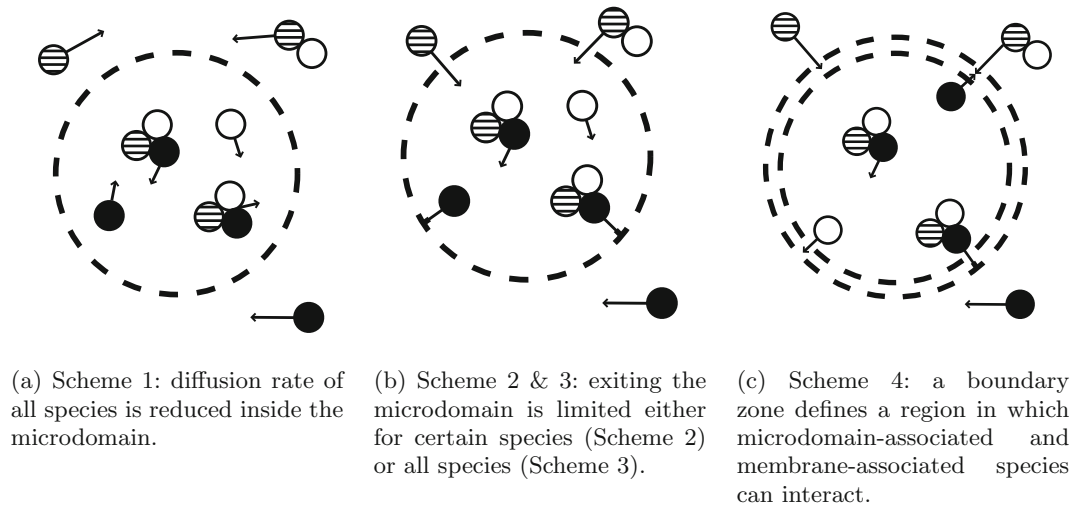


Fig. 2. The four diffusion schemes investigated in this paper: solid black discs denote α subunits and striped and clear discs denote, respectively, β and γ subunits. The dashed line represents the boundary of the microdomain.

Regulatory T cells (T_{reg} cells) are a particular subset of the T cell population that are influenced by IL-2 and related cytokines. In mice which do not make IL-2 or the IL-2R α subunit, T_{reg} cells disappear after 8 weeks of age. Those which lack IL-2R β also have severely reduced T_{reg} counts and those lacking the γ -chain produce no T_{reg} cells at all [5].

IL-2 receptors are being considered as a possible therapeutic target to stimulate T cell populations in patients who are immunodeficient due to HIV/AIDS [22], or to block overproliferation of T cells in leukaemia [23]. An important consideration is that IL-2 has a high rate of systemic depletion and affects a large number of cell types. For that reason, high doses are currently required in therapy which can be toxic or lethal. Fallon & Lauffenburger used a computational model to identify changes to intracellular receptor–ligand binding affinities that increased T cell sensitivity to IL-2 and thus design a mutant which could be used at a lower dose [24]. The model, however, assumed that the receptors for IL-2 were pre-formed. Optimising the formation of the receptor could lead to higher sensitivity to ligand and enable lower therapeutic doses.

4 Method

We construct a computational framework to examine the effect of varying quantitative and qualitative characteristics of the membrane environment on a ternary protein-protein interaction system. The reaction-diffusion system models the formation of IL-2 receptors in two stages. First, the β and γ subunits form a dimer (the medium-affinity receptor), subsequently the dimer binds to the α subunit to form the high-affinity $\alpha\beta\gamma$ receptor. The membrane is represented by a rectangular grid and the proteins and complexes follow a random walk trajectory.

In the following subsections we define four qualitatively distinct diffusion schemes, each of which is based on hypotheses raised in the experimental literature (see Fig. 2).

4.1 Reduction in rate of diffusion within microdomains

In Scheme 1, a discretised membrane is uniformly seeded with subunit monomers and they are allowed to diffuse based on the values of the diffusion rate, D at their location (see Fig. 2(a)). The value of D is lower within microdomains than in the remaining membrane. If two subunits which can bind together to form a complex are positioned on the same grid point (pixel) then they may react together at a fixed rate. We vary the microdomain radii and total microdomain

Table 1. The probability, under diffusion schemes 2, 3 and 4, that a diffusing protein or protein complex will be allowed into or out of a microdomain. A value of 1 shows that the protein may diffuse freely across the boundary. The probability p , $0 \leq p \leq 1$ denotes the strength of affinity for a microdomain or for the membrane. For the case $p = 0$, a protein or complex is irreversibly trapped in its current compartment (membrane or microdomain).

| | α | β | γ | $\beta\gamma$ | $\alpha\beta\gamma$ |
|---------------|----------|---------|----------|---------------|---------------------|
| Scheme 2: in | 1 | 1 | 1 | 1 | 1 |
| Scheme 2: out | p | 1 | 1 | 1 | p |
| Scheme 3: in | 1 | 1 | 1 | 1 | 1 |
| Scheme 3: out | p | p | p | p | p |
| Scheme 4: in | 1 | p | p | p | p |
| Scheme 4: out | p | 1 | 1 | 1 | p |

coverage and measure the number of monomers and complexes over time. We ran simulations until the number of protein complexes reached an approximate equilibrium and tested total microdomain coverage of 0%, 10%, 25% and 50% of the membrane and microdomain radii of 1, 2, 3, 4, 5 and 6 pixels.

4.2 Protein species with affinity to microdomain

Experimental studies indicate that membrane-bound proteins may have different affinities to microdomains, in that some species cluster together with saturated-chain lipids while others do not. We model this by defining probability values which dictate whether, on an attempt to move from a microdomain region to a membrane region, the move is permitted. Thus, a value of 0 means that the protein cannot cross the boundary, whereas a value of 1 means that there is no constraint on diffusion.

Ellery and Nicholls [25] hypothesise a mechanism whereby the α subunit segregates preferentially to the microdomain region. They propose that when subunits are segregated into microdomains, the microdomain radius is key in allowing or preventing formation of the trimeric receptor complex: small microdomains mean that α subunits can more easily interact with β and γ subunits at the boundary, but trimer formation would be inhibited by large microdomains. The sorting of α subunits to microdomains is also supported by the experimental results of Marmor et al. [20]

We investigated two diffusion schemes (see Fig. 2(b)): in Scheme 2 we define an affinity of the α subunit (and any complexes which include it) for the microdomain, but no affinity for the remaining subunits (see Table 1). In Scheme 3 we apply an affinity for microdomain regions to all diffusing species. In these two schemes all diffusing species are free to enter the microdomains. We maintained microdomain coverage at 25%, and instead tested affinity values of $p = 0, 0.2, 0.5, 0.8$ and 1, and varied microdomain radii as in the previous case.

4.3 Proteins interact in boundary zone

To simulate the case where protein species are segregated into microdomain and membrane regions we modified the simulation to include a boundary zone of 1 pixel beyond the edge of the microdomain (Scheme 4). Both microdomain-associated and membrane-associated proteins can diffuse freely into this zone, but if proteins attempt to diffuse further into or further out of the microdomain area they can only do so with a fixed probability as before. The probabilities for each protein species are shown in Table 1. This scheme more closely matches the hypothesis of Ellery and Nicholls [25], in which constituent components of the signalling receptor are segregated by the microdomains and can only interact in a boundary region.

In these simulations, we again maintained a constant microdomain fraction of 25% and varied the microdomain or radii, and the conditions on the boundary.

4.4 Simulation method

The simulation uses an implementation of the Gillespie algorithm [26] to select which event will occur next and the waiting time between each event. Protein and complex locations are encoded by a rectangular matrix X_n ; $X_n(\mathbf{i}) \in \mathbb{N}$, where the value of n encodes the particular species of protein or protein complex and the vector \mathbf{i} gives the position. The value of each element $X_n(\mathbf{i})$ is the number of proteins or complexes at that position. A second matrix D ; $D(\mathbf{i}) \in \mathbb{R}$ determines the relative diffusion rates at different spatial locations \mathbf{i} , representing the location of microdomains. The rate of diffusion of all species is reduced inside microdomains.

The membrane grid is initially seeded with proteins of different species distributed randomly. More than one protein of any species may occupy the same pixel. The radius, r of the microdomain is specified for each simulation. In placing the microdomains, a centre point (x_0, y_0) is chosen uniformly at random in two dimensions and then the surrounding pixels (x_i, y_i) are marked as within a microdomain if $(x_i - x_0)^2 + (y_i - y_0)^2 \leq r^2$.

The model uses the Gillespie algorithm direct method to calculate the order and time at which events take place. All events have an associated rate and at each ‘Gillespie step’ one event is chosen at random according to the relative value of its rate. The time increment is dependent on the sum of all event rates. We first calculate a real value R_1 in the interval $[0,1]$. Then let the sum S of all event rates be:

$$S = \sum_{p_D} \sum_{\mathbf{i}} X_{p_D}(\mathbf{i}) \cdot D(\mathbf{i}) + \sum_{p_{m_1}, p_{m_2}} \sum_{\mathbf{i}} k_c X_{p_{m_1}}(\mathbf{i}) \cdot X_{p_{m_2}}(\mathbf{i}) + \sum_{p_C} \sum_{\mathbf{i}} k_d X_{p_C}(\mathbf{i}). \quad (1)$$

Where p_D are the protein species diffusing in the membrane, k_c is the rate of complex formation for each pair of complex components p_{m_1} and p_{m_2} occupying the same grid point, p_C are the protein complexes and k_d is the rate of complex decay. From this we calculate the timestep $\Delta t = -\frac{\log(R_1)}{S}$.

After incrementing the timestep, we choose an event to occur by choosing a second uniform random number, R_2 in the interval $[0,1]$. Then, if $s(i)$ is the rate at which event i occurs such that $\sum_i s(i) = S$, we choose event n to occur if:

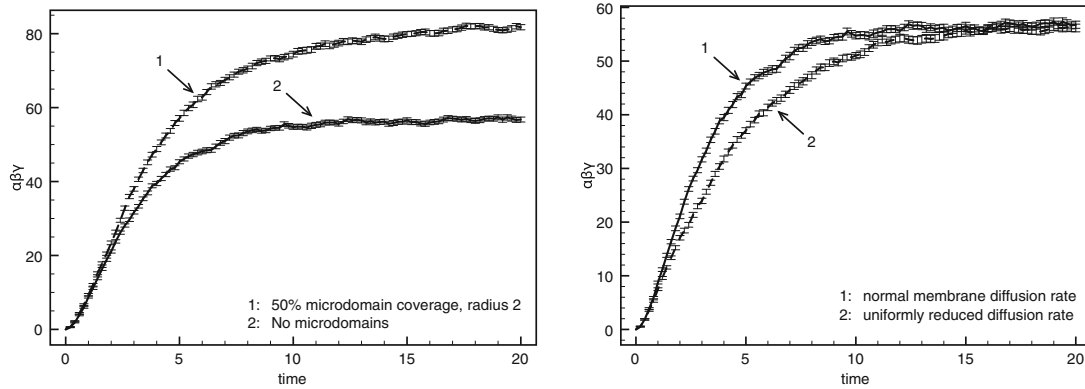
$$\begin{aligned} \sum_{i=1}^{n-1} s(i) < R_2 S \leq \sum_{i=1}^n s(i), n \geq 2 \\ 0 < R_2 S \leq s(1), n = 1. \end{aligned} \quad (2)$$

Events in the simulations include: movement of proteins and complexes to adjacent grid points; formation of a complex from subunits situated on the same pixel; and decay of a complex to its constituent subunits. Movement to an adjacent pixel is chosen uniformly at random from the four neighbouring pixels and the space has periodic boundary conditions. In Schemes 2–4 a move is proposed but only accepted with probability p determined by the affinity of the protein species. If the move is rejected then the time is incremented but the protein remains on the same pixel.

For the results shown, simulations were run on a square grid with 2500 pixels, with 600 of each of the monomeric subunits α , β , and γ . The rate of diffusion of all species (proteins and complexes) was set to 4 diffusion steps per time-unit in the membrane and 1 diffusion step per time-unit in the microdomains. The values for k_c and k_d were 1 and 0.5 respectively. Simulations were run until the timepoint $t = 20$ and repeated 100 times for each parameter set.

5 Results

We constructed stochastic simulations of a ternary protein reaction-diffusion system and evaluated the influence of small microdomains in which diffusion was slowed. We also tested the effect of defining degrees of affinity between diffusing species and microdomains; either having affinity for a single protein species, all protein species or segregating protein species so that protein-protein interactions are confined to a boundary zone.



(a) The number of trimeric receptors formed plotted against time, averaged over 100 runs with protein diffusion slowed inside the microdomains.

(b) The number of receptors formed over time for the case where either there are no microdomains or the entire membrane has a reduced diffusion rate.

Fig. 3. Plots of simulation output for Scheme 1 comparing reduced diffusion rate in microdomains with uniformly reduced diffusion rate. Error bars show standard error of the mean.

5.1 Presence of microdomains increases equilibrium number of trimers

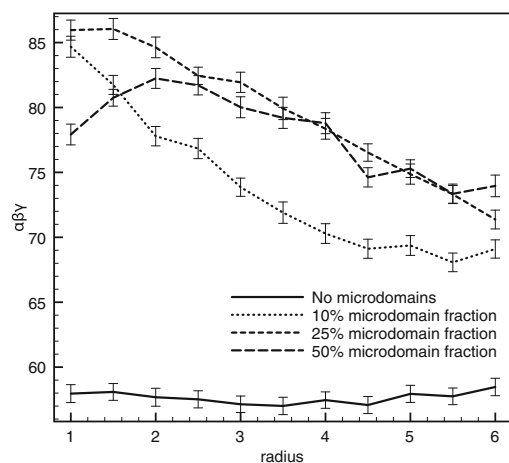
Figure 3(a) shows the average time evolution of the Scheme 1 simulation for microdomains of radius 2. The presence of microdomains in which diffusion is slowed increases both the rate of $\alpha\beta\gamma$ trimer formation and the equilibrium number of trimers. For comparison, Fig. 3(b) shows the time evolution where the diffusion rate is reduced to the microdomain diffusion rate across the entire membrane. In this case, the equilibrium outcome is unaffected but the rate of trimer formation is slowed.

We ran the same scheme for a range of microdomain radii and microdomain fraction values. The effect of varying these parameters on the equilibrium number of trimeric complexes is shown in Fig. 4(a). For all values that we tested, the presence of microdomains increased the number of trimers formed at $t = 20$. For microdomain coverage of 10% or 25%, the increase in trimer formation was highest for the smallest microdomain radii. At 50% microdomain coverage, smaller microdomains were also favoured, but the results indicate an ‘optimum’ microdomain radius of 2 pixels.

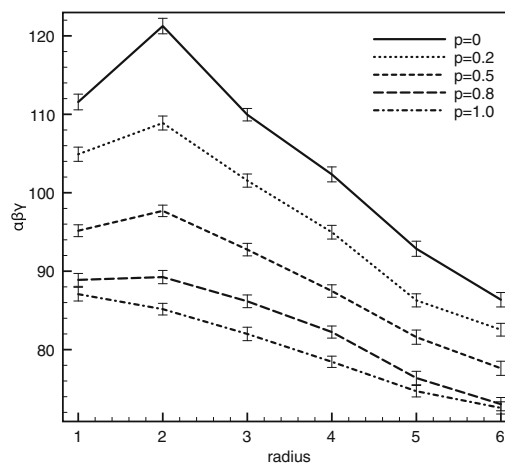
Although in most of the simulations we incremented the microdomain radius in whole pixels, we re-ran this simulation with fractional radii to check the value for the radius of 1 pixel and 50% microdomain fraction was not an anomaly. Although the radius is a non-integer, the microdomains are still discrete since pixels are included based on satisfaction of the inequality $(x_i - x_0)^2 + (y_i - y_0)^2 \leq r^2$ as in Sec. 4.4. The greatest number of trimers formed at equilibrium was obtained when the membrane microdomain fraction was at 25% and the microdomain radius was 1.5 pixels.

5.2 Microdomain affinity amplifies increase in equilibrium state

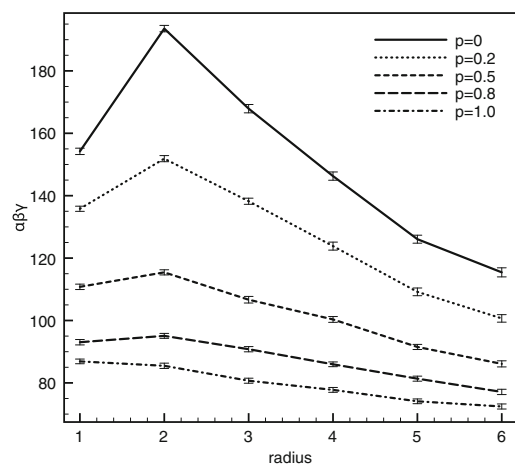
We tested five values of microdomain affinity by imposing a probability that a diffusion step will be accepted or rejected when a diffusing species attempts to move out of a microdomain region into the membrane. Figure 4(b) shows the equilibrium number of trimers formed in Scheme 2 with 25% microdomain coverage, where only the α component and the $\alpha\beta\gamma$ trimer have affinity for the microdomains. As in the results for Scheme 1, it implies an optimal microdomain radius of 2 pixels for almost all affinity values. As microdomain affinity is increased, the equilibrium number of trimeric complexes also increases dramatically. In Fig. 4(c) the results for Scheme 3 – where all component proteins and protein complexes have a microdomain affinity – are similar



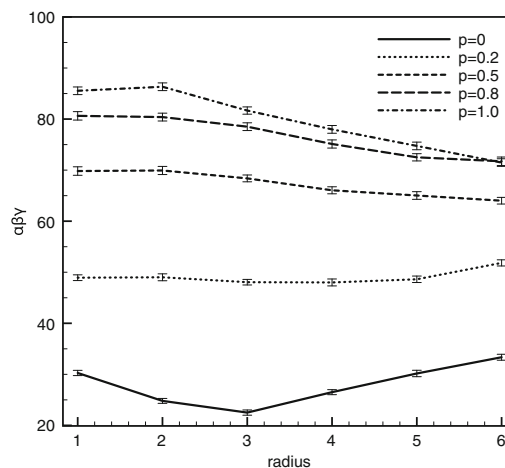
(a) Average number of trimers in the simulation at $t = 20$ plotted against microdomain radius, for four different values of microdomain coverage (Scheme 1).



(b) Trimers in at $t = 20$ where α subunits have affinity for microdomains (Scheme 2).



(c) Trimers at $t = 20$ where all subunits have affinity for microdomains (Scheme 3).



(d) Trimers at $t = 20$ where protein interactions are localised to microdomain boundaries (Scheme 4).

Fig. 4. Plots showing the average number of trimers formed in equilibrium for all four diffusion schemes. In plots (b)–(d), microdomain coverage is 25%. Values are averaged over 100 simulation runs and error bars show the standard error of the mean.

to those for Scheme 2, but the increase in the number of trimers is amplified to an even greater extent.

5.3 Confinement of protein-protein interaction to microdomain boundary inhibits receptor formation

Figure 4(d) shows the results for Scheme 4, where proteins and complexes can diffuse uninhibited into a boundary zone 1 pixel thick around the microdomains but diffusion from the boundary zone either into microdomains or out of microdomains is subject to affinity constraints. In the results shown, α proteins and $\alpha\beta\gamma$ trimers have affinity for microdomains given by the value

of p , whereas the remaining species have affinity for the membrane and are prevented from entering the microdomains.

In this case, as would be expected, stronger affinity values segregate the components of the receptor more severely and lead to lower numbers of trimers formed in equilibrium. For the strongest affinity values $p = 0$ and $p = 0.2$, the number of receptors formed is lower than the system with no microdomains. The effect of varying the microdomain radius depends on the strength of microdomain affinity. For strong affinity ($p = 0$), the results suggest that microdomain radii of 3 pixels lead to the strongest segregating effect and the lowest number of trimeric complexes in equilibrium. For weak affinity ($p \leq 0.5$), however, microdomain radii of 2 or 3 pixels results in a comparatively high number of trimers formed in equilibrium.

6 Discussion

In this study, we have created an *in-silico* model of a cell membrane, incorporating compartmentalised diffusion processes, protein-protein interactions and membrane-protein affinity terms. Using this model, we investigated four qualitatively distinct hypotheses for the role of microdomain-mediated protein sorting on the formation of trimeric protein receptor complexes.

The simulation results show that the presence of microdomains with a reduced diffusion rate can increase the equilibrium number of trimeric receptor complexes in the cell membrane. In the model, small microdomains maximise receptor formation. For relatively high (50%) membrane microdomain coverage, the results indicate the existence of an ‘optimal’ microdomain radius of around 2 pixels. As observed microdomains are indeed small (10–100nm), it could be explored whether there is an evolutionary mechanism selecting for microdomain size. The existence of optimal microdomain radii to facilitate protein-protein interactions is in agreement with the results of Nicolau *et al.* [14], but we saw this property for static rather than mobile microdomains. The reason for a difference in outcomes for a model based on binding and dissociation rather than protein-protein collision could be the number of distinct components needed to form the complex, meaning concentrating the subunits in a small area is more important.

An increase in the number of receptors when there was a high affinity for all protein species was unsurprising, but receptor numbers also increased when only the α subunit had increased affinity for the microdomains. This result could suggest that modifying protein subunits, by creating analogs or posttranslational modification, could be used to augment receptor complex formation. Also, since IL-2 and IL-15 share the $\beta\gamma$ complex, modifying one of the α subunits to increase its affinity for microdomains could be a potential tool to alter T cell fate by promoting the IL-2 signalling pathway over the IL-15 pathway or vice versa.

Finally the results from the Scheme 4 simulations show a role for the segregating effect of microdomains. Ellery & Nicholls [25] suggest that larger microdomains would inhibit receptor formation and small microdomains would promote it. In contrast, our results indicate that the strength of the segregating effect (microdomain affinity) is key in determining the number of receptors formed and that microdomain sizes that promote the greatest number of receptors when proteins have a low microdomain affinity can result in the lowest number of receptors when they have a high microdomain affinity.

Several limitations of the model should be addressed. First, the size of the simulated membrane is relatively small in order to generate a sufficient range of results in a short amount of time. The results of larger simulations (with 4×10^4 pixels) of Scheme 1 were similar to results shown here. Secondly, parameters were chosen for simplicity rather than biological accuracy so results should be interpreted as a proof of principle rather than predictive of *in vivo* behaviour of the IL-2 receptor. The diffusion rate, particularly, was set equal for all proteins and protein complexes. In future work, we plan to make more biologically relevant predictions by using experimentally determined diffusion rates for all species. The model also did not limit the occupancy of each pixel; in later models we intend to investigate the limitations imposed by crowding inside microdomains. Finally, we have considered the formation of the IL-2 receptor in this model, but no ligand-receptor binding dynamics. We hope to address this mechanism and its influence on the proliferative response in future work.

In conclusion, we have discussed a model of IL-2 receptor formation in the T cell membrane in relation to the presence of microdomains in which diffusion is slowed and for which the diffusing species may have a particular affinity. While remaining agnostic to the mechanisms contributing to the formation of microdomains and indeed their prevalence *in vivo*, we have demonstrated that the presence of small membrane compartments with these characteristics can promote the formation of receptors relevant to signalling and suggested ways in which this could be therapeutically exploited. In light of these results, we think that spatial heterogeneity in the membrane is an important factor to consider in constructing larger models which incorporate transmembrane signalling components.

EL is supported by an Engineering and Physical Sciences Research Council Research Studentship. AZ thanks L. Schimansky-Geier, with whom AZ was a PhD student in 1997–98, for many fruitful discussions and his great input in establishing AZ as a physicist.

References

1. K. Simons, E. Ikonen, *Nature* **387**, 569 (1997)
2. R. Xavier, T. Brennan, Q. Li, C. McCormack, B. Seed, *Immunity* **8**, 6 (1998)
3. A. Grakoui, S. Bromley, C. Sumen, M. Davis, A. Shaw, P. Allen, M. Dustin, *Science* **285**, 221 (1999)
4. T. Zech, C.S. Ejsing, K. Gaus, B. de Wet, A. Shevchenko, K. Simons, T. Harder, *EMBO J.* **28**, 5 (2009)
5. M.A. Burchill, J. Yang, K.B. Vang, M.A. Farrar, *Immunol. Lett.* **114**, 1 (2007)
6. S. Singer, G. Nicolson, *Science* **175**, 720 (1972)
7. F.M. Goñi, A. Alonso, L.A. Bagatolli, R.E. Brown, D. Marsh, M. Prieto, J.L. Thewalt, *Biochim. Biophys. Acta* **1781**, 665 (2008)
8. B.C. Lagerholm, G.E. Weinreb, K. Jacobson, N.L. Thompson, *Annu. Rev. Phys. Chem.* **56**, 309 (2005)
9. M.S. Turner, P. Sens, N.D. Socci, *Phys. Rev. Lett.* **95**, 16 (2005)
10. M. Venturoli, M.M. Sperotto, M. Kranenburg, B. Smit, *Phys. Rep.* **437**, 1 (2006)
11. S.A. Pandit, *Biophys. J.* **87**, 5 (2004)
12. H.J. Risselada, S.J. Marrink, *Proc. Natl. Acad. Sci. USA* **105**, 45 (2008)
13. G. Nudelman, M. Weigert, Y. Louzoun, *Mol. Immunol.* **46**, 15 (2009)
14. D.V. Nicolau, K. Burrage, R.G. Parton, J.F. Hancock, *Mol. Cell. Biol.* **26**, 1 (2006)
15. A. Bodnár, E. Nizsalóczki, G. Mocsár, N. Szalóki, *Immunol. Lett.* **116**, 117 (2008)
16. T. Taniguchi, *Science* **268**, 251 (1995)
17. J. Matkó, A. Bodnár, G. Vereb, L. Bene, G. Vámosi, *Eur. J. Biochem.* **269**, 1199 (2002)
18. G. Vereb, J. Matkó, G. Vámosi, S.M. Ibrahim, E. Magyar, S. Varga, J. Szöllosi, A. Jenei, R. Gáspár, T.A. Waldmann, S. Damjanovich, *Proc. Natl. Acad. Sci. USA* **97**, 11 (2000)
19. J. Goebel, K. Forrest, L. Morford, T.L. Roszman, *J. Leukoc. Biol.* **72**, 1 (2002)
20. M. Marmor, M. Julius, *Blood* (2001)
21. A. Ma, R. Koka, P. Burkett, *Annu. Rev. Immunol.* **16**, 33 (2000)
22. H.P. Kim, J. Imbert, W.J. Leonard, *Cytokine Growth Factor Rev.* **17**, 349 (2006)
23. T.A. Waldmann, *J. Clin. Immunol.* **22**, 2 (2002)
24. E.M. Fallon, D.A. Lauffenburger, *Biotechnol. Prog.* **16**, 5 (2000)
25. J.M. Ellery, P.J. Nicholls, *Immunol. Cell. Biol.* **80**, 4 (2002)
26. M. Gibson, J. Bruck, *J. Phys. Chem. A* **104**, 1876 (2000)